

## Targeting Radiation-Induced G<sub>2</sub> Checkpoint Activation with the Wee-1 Inhibitor MK-1775 in Glioblastoma Cell Lines

Bhaswati Sarcar<sup>1</sup>, Soumen Kahali<sup>1</sup>, Antony H. Prabhu<sup>1</sup>, Stuart D. Shumway<sup>2</sup>, Yang Xu<sup>2</sup>, Tim Demuth<sup>2</sup>, and Prakash Chinnaiyan<sup>1</sup>

### Abstract

The purpose of this study was to determine the capacity of MK-1775, a potent Wee-1 inhibitor, to abrogate the radiation-induced G<sub>2</sub> checkpoint arrest and modulate radiosensitivity in glioblastoma cell models and normal human astrocytes. The radiation-induced checkpoint response of established glioblastoma cell lines, glioblastoma neural stem (GNS) cells, and astrocytes were determined *in vitro* by flow cytometry and *in vivo* by mitosis-specific staining using immunohistochemistry. Mechanisms underlying MK-1775 radiosensitization were determined by mitotic catastrophe and  $\gamma$ H2AX expression. Radiosensitivity was determined *in vitro* by the clonogenic assay and *in vivo* by tumor growth delay. MK-1775 abrogated the radiation-induced G<sub>2</sub> checkpoint and enhanced radiosensitivity in established glioblastoma cell lines *in vitro* and *in vivo*, without modulating radiation response in normal human astrocytes. MK-1775 appeared to attenuate the early-phase of the G<sub>2</sub> checkpoint arrest in GNS cell lines, although the arrest was not sustained and did not lead to increased radiosensitivity. These results show that MK-1775 can selectively enhance radiosensitivity in established glioblastoma cell lines. Further work is required to determine the role Wee-1 plays in checkpoint activation of GNS cells. *Mol Cancer Ther*; 10(12); 2405–14. ©2011 AACR.

### Introduction

Radiation therapy remains a primary treatment modality for glioblastoma. Despite relatively large radiation doses, tumors recur at the original site in more than 80% of cases (1). This local recurrence within the initial radiation treatment volume indicates that glioblastoma is extremely radioresistant, providing rationale for the active development of radiosensitizers in this tumor. Although several lead compounds have been identified and are under clinical investigation, a potential limitation to these agents is that their effects on normal tissue remains unclear; therefore, the combination of these agents with radiation may result in simple dose escalation rather than a clinically meaningful enhancement of therapeutic ratio. Therefore, identifying agents with the capacity of modulating tumor-specific radiation response holds promise in improving clinical gains in glioblastoma.

Immediately following radiation-induced DNA damage, cells undergo a cell-cycle arrest to allow for repair before continued proliferation. Typically, this is manifest as a G<sub>1</sub> phase arrest activated in a p53-dependent manner. However, as a significant proportion of tumors have abnormalities in the p53 pathway, an alternate G<sub>2</sub> checkpoint is activated in a p53-independent manner. A critical downstream mediator of this checkpoint is the Wee-1 kinase (2). Wee-1 is phosphorylated at S549 by several kinases, including Chk1, followed by binding to 14-3-3 proteins that lead to Wee-1 stabilization. The phosphorylated and stable Wee-1 increases the level of inactivated phosphorylated-CDC2, leading to G<sub>2</sub> phase checkpoint activation, thereby preventing the damaged cells from entering into premature mitosis without repairing the DNA (2–7).

On the basis of the differential radiation-induced checkpoint activation between normal tissue and p53-inactivated tumors, targeting proteins involved in the p53-independent G<sub>2</sub> checkpoint response represents an attractive strategy for tumor-specific radiosensitization (3). A high-throughput screening conducted on a chemical compound library identified MK-1775 (Merck Research Laboratories) as a potent and selective small-molecule inhibitor of the Wee-1 kinase (8). Preclinical studies have shown the capacity of MK-1775 to enhance the cytotoxicity of several chemotherapeutic agents, including gemcitabine, carboplatin, cisplatin, and 5-fluorouracil both *in vitro* and *in vivo*. Currently, MK-1775 is being actively investigated in early-phase clinical trials.

Historically, p53 inactivation has been considered as a classical lesion in low-grade astrocytoma and secondary

**Authors' Affiliations:** <sup>1</sup>Radiation Oncology and Experimental Therapeutics, H. Lee Moffitt Cancer Center, Tampa, Florida; and <sup>2</sup>Department of Oncology, Merck Research Laboratories, Upper Gwynedd, Pennsylvania

**Note:** Supplementary data for this article are available at Molecular Cancer Therapeutics Online (<http://mct.aacrjournals.org>).

**Corresponding Author:** Prakash Chinnaiyan, Assistant Member, Department of Radiation Oncology and Experimental Therapeutics, H. Lee Moffitt Cancer Center and Research Institute, SRB3, 12902 Magnolia Drive, Tampa, FL 33612. Phone: 813-745-3425; Fax: 813-745-3829; E-mail: [prakash.chinnaiyan@moffitt.org](mailto:prakash.chinnaiyan@moffitt.org)

doi: 10.1158/1535-7163.MCT-11-0469

©2011 American Association for Cancer Research.

glioblastoma but infrequent in primary human glioblastoma. However, recent sequencing of human glioblastoma identified an unexpectedly frequent inactivation of p53 by DNA mutation (9). Furthermore, recent data presented by The Cancer Genome Atlas Research Network identified altered p53 signaling in 87% of glioblastoma (10), supporting the potential of this pathway to serve as a tumor-specific therapeutic target in a significant proportion of glioblastoma (8, 11). In addition, recent reports suggest that the Wee-1 kinase is overexpressed in glioblastoma and correlates with survival (12), emphasizing its importance to serve as a molecular target in this malignancy. In this study, we show the capacity of the Wee-1 inhibitor MK-1775 to modulate radiation response in glioblastoma models, supporting the further investigation of this combination in the context of a clinical trial.

## Materials and Methods

### Cell lines and treatment

The established human glioblastoma cell lines U251, U87, and T98G were obtained from American Type Culture Collection and grown in RPMI-1640 (Gibco) and Eagle's Minimum Essential Medium with Earle's salt and L-glutamine (Cellgro), respectively, and supplemented with heat-inactivated FBS (Gibco). Normal human astrocytes (NHA; Clonetics, Lonza) were grown in and maintained according to the manufacturer's instructions. Glioblastoma neural stem cell (GNS) lines G179 and G144 (p53 mutant) were provided by Dr. Austin Smith, Wellcome Trust Centre for Stem Cell Research, University of Cambridge, Cambridge, UK (13), and distributed by BioRep. Undifferentiated GNS cell expansion was carried out according to manufacturer's instructions. Cell line authentication was not carried out by authors within the last 6 months. MK-1775 was provided by Merck Research Laboratories.

### Irradiation

Cell lines were irradiated *in vitro* using an XRad 160 X-ray source (Precision X Ray Inc.) at 160 kV at a dose rate of 2.5 Gy/min. For *in vivo* irradiation, mice were anesthetized using ketamine/xylazine and placed in well-ventilated custom jigs (Precision X-Ray), allowing for local delivery of radiation using an XRad 320 X-ray source (Precision X Ray) at 320 kV at a dose rate of 289.8 cGy/min.

### Clonogenic assay

Cell survival was defined using a standard clonogenic assay. Cultures were trypsinized to generate a single-cell suspension and cells were seeded into 6-well tissue culture plates. Similar methods were used for GNS cells; however, plates were coated in laminin and maintained in serum-free media as described above. Plates were then treated as described 16 hours after seeding to allow cells to attach. Colonies were stained with crystal violet 10 to 14 days after seeding, the number of colonies containing at least 50 cells counted, and surviving fractions were calculated. Unless otherwise stated, cells were treated with

MK-1775 or vehicle control a total of 24 hours, beginning 6 hours before irradiation. A dose enhancement factor (DEF) was calculated to quantify differences between survival curves. The DEF was defined as the radiation dose resulting in a 10% survival rate divided by the MK-1775-treated radiation dose resulting in a 10% survival rate. To extend the clonogenic assay to normal astrocytes, a hybrid clonogenic assay was developed. Similar methods were used as the traditional clonogenic assay; however, cells were seeded in 12-well tissue culture plates in higher densities, and cells were counted in duplicate using a Beckman Coulter counter (Beckman Coulter, Inc.) 5 days following irradiation.

### Cell-cycle phase analysis

After described treatment, cells were prepared for fluorescence-activated cell sorting (FACS) to assess the relative distribution in the respective phases of the cell cycle. Cells were pelleted by centrifugation, resuspended in PBS, fixed in 70% ethanol, and stored at  $-20^{\circ}\text{C}$ . Immediately before flow cytometry, the cells were washed in cold PBS and subsequently permeabilized with PBS containing 1 mg/mL propidium iodide (Sigma-Aldrich), 0.1% Triton X-100 (Sigma-Aldrich), and 2 mg DNase-free RNase (Sigma-Aldrich) at room temperature and incubated in the dark for 30 minutes at  $4^{\circ}\text{C}$ . Samples were measured (15,000 events collected from each) in a BD Pharmingen FACScan (BD Pharmingen). To determine the percentage of cells in mitosis, cells were fixed with ethanol, and dual staining of cells was done with propidium iodide and an anti-phospho-Histone H3 (pS10)-specific antibody conjugated with Alexa Fluor 488 (Cell Signaling).

### Immunoblot analysis

Total proteins were prepared from whole-cell lysates. Exponentially growing cells were dissolved in ice-cold cell lysis buffer as described previously (14). The blot was analyzed with mouse monoclonal antibodies against human anti-CDC2 (1:2,000; BD Biosciences), human anti-CDC2pY15 (1:250; BD Biosciences), rabbit polyclonal antibodies against human anti-Wee-1 (1:800; Cell Signaling Technologies), and mouse anti- $\beta$ -actin (1:20,000; Sigma-Aldrich). Secondary antibodies conjugated to horseradish peroxidase (GE Healthcare) were used, and chemiluminescence (Thermo Fisher Scientific) was used for detection.

### Mitotic catastrophe

Cells were seeded into Lab-Tek II tissue culture slides (Thermo Fisher). Cultures were fixed with 4% paraformaldehyde, permeabilized with 0.2% Triton X-100, and blocked with 1% bovine serum albumin in PBS and then stained overnight at  $4^{\circ}\text{C}$  with mouse anti- $\alpha$ -tubulin antibody (Sigma-Aldrich). Cells were washed with 1% bovine serum albumin, stained with secondary antibody (Alexa Fluor 488 goat antimouse IgG; Invitrogen) for 2 hours and mounted with anti-fade containing 4',6-diamidino-2-phenylindole (Invitrogen). A minimum of 200 cells were

analyzed and scored for each treatment group on a Zeiss upright fluorescent microscope. The criterion for defining cells undergoing mitotic catastrophe was the presence of nuclei fragmented with 2 or more lobes within a single cell.

### MK-1775 pharmacokinetics

These studies were conducted in strict accordance to guidelines described by the Institutional Animal Care and Use Committee of University of South Florida, Tampa, FL. MK-1775 (60 mg/kg) dissolved in 0.5% methylcellulose (Sigma-Aldrich) solution was administered to 4- to 6-week-old athymic *nu/nu* mice (Charles River Laboratories) via oral gavage and blood samples obtained using the submandibular bleed technique at stated time points. Samples were placed in microcentrifuge tubes preloaded with 30  $\mu$ L of citrate buffer (Sigma-Aldrich) and kept on ice, then stored at  $-20^{\circ}\text{C}$  until analysis. MK-1775 in 10  $\mu$ L mouse blood samples was extracted using protein precipitation in the presence of stable isotope-labeled internal standard. After vortexing and centrifugation, the supernatant was analyzed using high-performance liquid chromatography (HPLC) coupled with tandem mass spectrometry (MS-MS) on an API4000 using a Turbo Ionspray source under the positive ionization mode with multiple reaction monitoring (MRM) to detect the analyte precursor  $\rightarrow$  product ion transitions.

### In vivo tumor growth delay

Subcutaneous xenograft tumors were formed by injection of U251 cells ( $5 \times 10^6$ ) in the hind flank of 4- to 6-week-old athymic *nu/nu* mice (Charles River Laboratories). When tumors grew to a mean volume of about 150  $\text{mm}^3$ , mice were randomized to 1 of the following 4 treatment groups (7 mice per treatment group): vehicle control, MK-1775, fractionated radiation, or MK-1775 + fractionated radiation. MK-1775 (60 mg/kg twice a day in 0.5% methyl cellulose solution) was administered orally over a 3-day period. Irradiated mice (2 Gy/d  $\times$  3 days) were anesthetized and immobilized in a custom jig with a left flank shield that allowed for the localized irradiation of the implanted tumors. Animals were monitored and tumor volumes calculated ( $L \times W \times W$ )/2 three times a week. Mice were sacrificed when the tumor volume of an individual mouse in a treatment arm reached a dimension of 1,000  $\text{mm}^3$  or larger or developed clinical signs.

### In vivo mitotic ratio

After observing the presence of a palpable tumor ( $>500 \text{mm}^3$ ), mice were randomized into 2 groups: radiation alone (6 Gy) and MK-1775 (60 mg/kg) + radiation and treated as described above. At the stated times, animals were sacrificed and tumors were removed, formalin fixed and paraffin embedded. Immunohistochemical staining was conducted to determine the mitotic ratio using a phospho-histone H3 (pS28) antibody (Epitomics). Samples were then quantified using an automated system. In brief, histology slides stained with phospho-histone H3

were scanned using the Aperio ScanScope XT with a  $200\times/0.8$  numerical aperture objective lens via Basler tri-linear-array detection. Image analysis was conducted using an Aperio Nuclear v9.1 algorithm using optimized thresholds. The percentage of reactivity was quantified by the number of cells exhibiting darkest positive stain as a percentage of total tumor cell count. The staining intensity was then thresholded using a dynamic range for each tissue section and tumor region individually. This algorithm was applied to the digital image of the entire slide to determine the percentage of positive staining by applicable area.

### Statistics

The statistical analysis was done for the described treatment conditions using the Student *t* test. A probability level of a value of  $P < 0.05$  was considered significant.

### Results

#### Independent cytotoxicity of MK-1775

Initial studies were conducted to determine the independent cytotoxicity of MK-1775 in glioblastoma cell lines. Clonogenic survival analysis following 24-hour exposure of graded concentrations of MK-1775 showed a similar cytotoxicity profile of MK-1775 in both U251 and T98G lines. Cells exposed to a 100 nmol/L concentration of MK-1775, which has been previously reported to achieve target engagement (8), resulted in minimal cytotoxicity, whereas 250 nmol/L concentrations resulted in approximately a 50% decrease in survival rate (Supplementary Fig. S1A). Continuous exposure to MK-1775 (100 nmol/L) for up to 72 hours did not significantly increase cytotoxicity (Supplementary Fig. S1B).

#### MK-1775 abrogates radiation-induced G<sub>2</sub> checkpoint arrest

Next, we evaluated the potential of MK-1775 to abrogate the radiation-induced G<sub>2</sub> cell-cycle arrest by FACS analysis. Exposing T98G to 6 Gy ionizing radiation resulted in an increase in G<sub>2</sub>-M arrest in a time course manner for up to 16 hours, followed by rapid normalization by 24 hours. Exposing cells to MK-1775 alone did not influence cell-cycle phase distribution (Supplementary Fig. S2). Exposing cells to MK-1775 6 hours before radiation attenuated G<sub>2</sub>-M phase accumulation in a dose-response manner [Fig. 1A;  $P = 0.001, 0.0009$  at 6 and 16 hours, in cells exposed to MK-1775 (250 nmol/L), respectively]. To separate cells in G<sub>2</sub> phase (4n) into the individual G<sub>2</sub> and M phase components, dual labeling was conducted with propidium iodide and phosphorylated histone H3, which is specifically expressed during the mitotic phase (5). Done as a function of time after irradiation, the progression of G<sub>2</sub> cells into M phase can be measured. As shown in Fig. 1B, exposing T98G to 6 Gy radiation resulted in a significant reduction in mitotic ratio, reflecting the onset of G<sub>2</sub> arrest. Pretreatment of cells with MK-1775 pushed G<sub>2</sub> phase cells into M phase

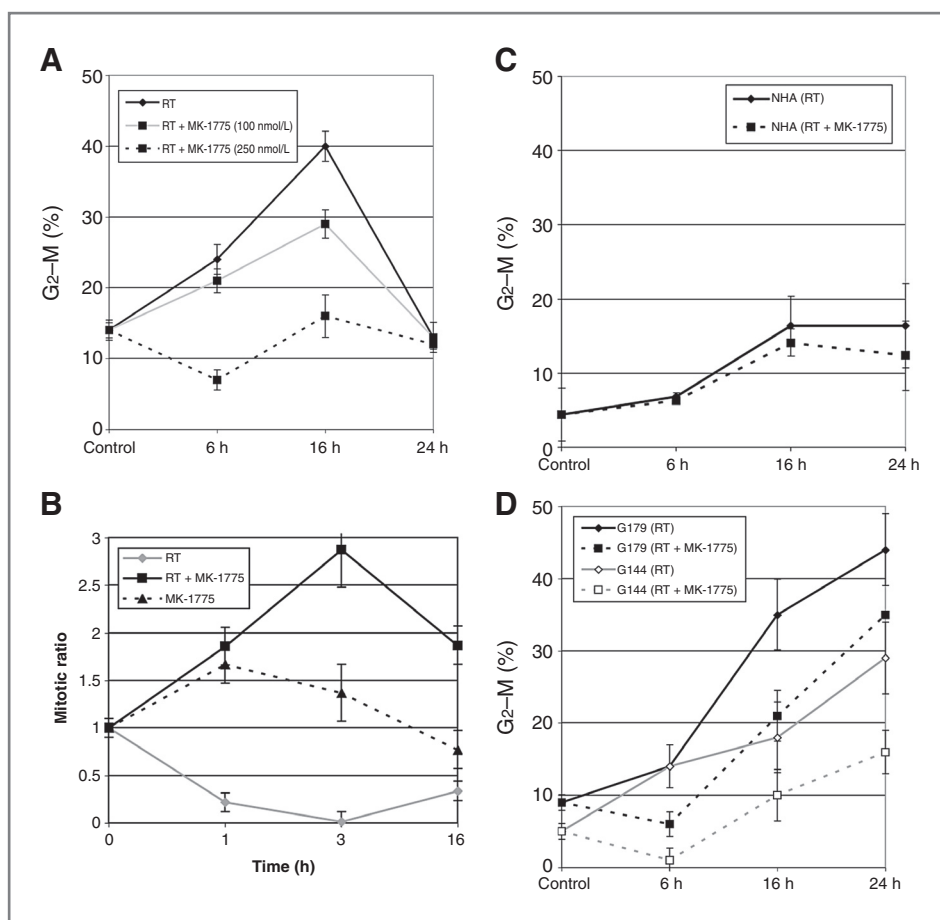


**Figure 1.** The influence of MK-1775 on radiation-induced G<sub>2</sub> checkpoint activation. T98G (A), NHAs (C), and the GNS (D) cells were treated with MK-1775 (250 nmol/L, unless otherwise noted) or vehicle control 6 hours before irradiation (RT; 6 Gy) and collected at specified time points for analysis of cell-cycle phase distribution by flow cytometry. Mean  $\pm$  SE of 3 independent experiments. B, mitotic ratio in T98G cells was determined using dual propidium iodide and phospho-histone H3 staining and calculated by the percentage of cells in M phase pre-/post-irradiation. Results are representative of 3 independent experiments; mean  $\pm$  SE.

following irradiation, as shown by an increased mitotic ratio, further supporting this potential of the compound of abrogating radiation-induced G<sub>2</sub> arrest (radiation vs. radiation + MK-1775:  $P = 0.001, 0.0005, \text{ and } 0.001$  at 1, 3, and 16 hours, respectively). Similar findings were observed in U251 and U87 cells (Supplementary Fig. S3). As a critical factor determining the clinical application of a putative radiosensitizer involves differential activity between normal and tumor cells, we expanded these studies to include NHAs. Astrocytes did show a modest accumulation in G<sub>2</sub>-M phase following irradiation; however, this was not significantly affected by MK-1775 (Fig. 1C;  $P = 0.76, 0.43, \text{ and } 0.25$  at 6, 16, and 24 hours, respectively).

It has recently been hypothesized that a small population of brain tumor cells within a tumor exhibit stem cell-like features, constituting a reservoir of self-sustaining cells with the exclusive ability to self-renew (15, 16). In addition to giving rise to the bulk of the tumor cells with more differentiated phenotypes and having a central role in tumorigenesis, these cells have also been implicated in radioresistance (17). Therefore, we extended our work to evaluate the capacity of MK-1775 to influence radiation response in GNS cell lines, using models described by Pollard and colleagues (13). Similar to the glioblastoma cell line T98G, GNS lines G179 and G144 showed an

accumulation in the G<sub>2</sub>-M phase following irradiation. However, unlike the established glioblastoma lines, where the G<sub>2</sub>-M phase fraction returned to baseline levels by 24 hours, the GNS lines showed a sustained arrest. Exposing cells to MK-1775 at a concentration of 250 nmol/L, which completely mitigated radiation-induced G<sub>2</sub>-M accumulation in T98G, did attenuate the initial accumulation of cells into G<sub>2</sub>-M phase (6 hours;  $P = 0.005$  and  $0.01$  in G144 and G179, respectively); however, this arrest was not sustained, with both GNS lines resuming G<sub>2</sub> phase accumulation at 16 and 24 hours (Fig. 1D).

#### MK-1775 attenuates radiation-induced phosphorylation of CDC2

The primary downstream mediator of Wee-1-induced G<sub>2</sub> phase arrest involves phosphorylation, and thereby inactivation, of the cyclin-dependent kinase CDC2 (7). Therefore, Western blot analysis was conducted to determine the potential of MK-1775 to inhibit CDC2 phosphorylation in our model. In T98G cells, increased phosphorylation of CDC2 was observed at 10 and 16 hours following 6 Gy irradiation. Exposing cells to MK-1775 (250 nmol/L) 6 hours before irradiation attenuated CDC2 phosphorylation, further supporting the role of MK-1775 in G<sub>2</sub> checkpoint abrogation (Fig. 2).

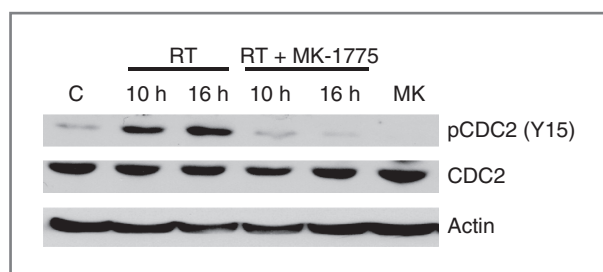


**Figure 2.** MK-1775 attenuates radiation-induced CDC2 phosphorylation. Tumor cell lysates from T98G cells exposed to vehicle control (C), MK-1775 (MK) alone (250 nmol/L, 16 hours), radiation alone (RT, 6 Gy), or combined with MK-1775 (250 nmol/L, 6 hours before RT) at the indicated times were resolved in SDS-PAGE and probed with specific antibodies against the indicated proteins. Results are representative of 2 independent experiments.

### MK-1775 enhances radiation-induced cell killing

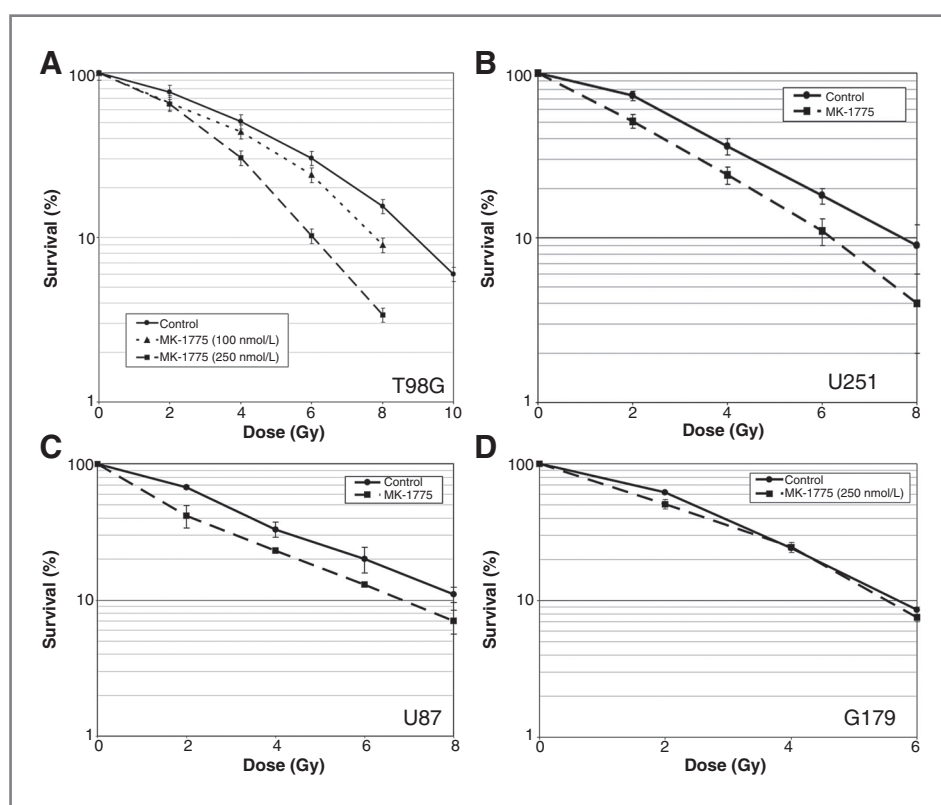
Given the role radiation-induced  $G_2$  arrest plays in DNA repair, we determined the effect of MK-1775 on radiosensitivity using the clonogenic assay. Exposure of T98G to 100 and 250 nmol/L MK-1775 6 hours before irradiation, which represent concentrations we established that lead to modest and complete abrogation of radiation-induced  $G_2$  arrest, respectively (Fig. 1A), resulted in a concentration-dependent increase in radiosensitivity with DEFs of 1.2 and 1.5, respectively (Fig. 3A). A similar DEF (1.2) was shown in U251 cells exposed

to MK-1775 (100 nmol/L; Fig. 3B). As a significant proportion of glioblastoma harbor mutations in genes involved in p53 signaling, apart from p53 itself (9, 10), we carried out similar experiments using the p53 wild-type glioblastoma line U87. Despite harboring wild-type p53, U87 also showed a similar enhancement in radiation response by MK-1775 (DEF = 1.2; Fig. 3C). Finally, we extended these investigations to GNS cells, which have been implicated in radioresistance. Unlike the established glioblastoma cell lines, despite showing an initial attenuation of radiation-induced  $G_2$ -M phase accumulation (Fig. 1D), radiosensitivity of the GNS cell line G179 was not enhanced when exposed to MK-1775 (Fig. 3D).

### MK-1775 attenuates recovery during fractionated radiation

As we have established that a concentration of 100 nmol/L MK-1775 results in both modest attenuation of radiation-induced  $G_2$  arrest (Fig. 1A) and enhanced radiosensitivity (Fig. 3A), yet had no independent cytotoxicity for up to 72 hours of exposure (Supplementary Fig. S1B), we extended our investigations to determine the capacity of MK-1775 to modulate the more clinically relevant approach of fractionated radiation using the clonogenic assay. For these studies, a recovery rate was calculated, which was obtained by dividing the percentage of cell survival following fractionated radiation (2 Gy fractions

**Figure 3.** The influence of MK-1775 on radiosensitivity in glioblastoma cell lines. Glioblastoma cell lines T98G (A; p53 mutant), U251 (B; p53 mutant), U87 (C; p53 wild-type), and GNS cell line G179 (D; p53 mutant) were plated, allowed to attach, and treated with either MK-1775 (100 nmol/L unless otherwise noted) or vehicle control for 6 hours pre-RT. Plates were replaced with fresh culture media after 24 hours, and surviving fractions were calculated 10 to 14 days following treatment, normalizing for the independent cytotoxicity of MK-1775. Mean  $\pm$  SE of 3 independent experiments.



delivered every 24 hours) by the percentage of cell survival following an equivalent dose of radiation delivered as a single fraction. As expected, on the basis of the capacity of repairing sublethal damage, T98G cells showed increased survival following fractionated radiation when compared with single fraction radiation, resulting in recovery rates of 1.22 and 1.64 at 4 and 6 Gy, respectively. Continuous exposure of T98G to MK-1775 during fractionated radiation completely abrogated recovery, resulting in a recover rate of 0.79 and 0.80 at 4 and 6 Gy, respectively (Fig. 4).

### Clonogenic hybrids

Although the clonogenic assay is the gold standard in measuring radiation-induced cell death, it can only be applied to cell lines that grow as colonies, limiting its application to several model systems, including normal astrocytes. Therefore, to gain insight into the potential of MK-1775 to enhance radiation response in astrocytes, and thereby mitigating its potential clinical application, a modified clonogenic hybrid assay was developed. This assay was initially optimized in T98G, which showed clear radiosensitization of MK-1775 using the traditional clonogenic assay. Simulating the treatment protocol used in the clonogenic assay, 12-well tissue culture plates were seeded as single cells, and viable cells were counted 5 days

following treatment. Consistent with the initial clonogenic survival data (Supplementary Fig. S1), 24-hour exposure of MK-1775 alone (250 nmol/L) resulted in approximately 60% of viable cells when compared with vehicle control (Supplementary Fig. S4). The combination of MK-1775 (250 nmol/L) with irradiation (6 Gy) resulted in 33% of viable cells when compared with cells exposed to radiation alone (6 Gy). A combination index (CI) was then calculated to normalize for the independent cytotoxicity of MK-1775 alone, by dividing the percentage of viable cells from the MK-1775/radiation combination (when compared with radiation alone) by the percentage of viable cells from MK-1775 alone (when compared with vehicle control). A CI = 1 would suggest no interaction between radiation and MK-1775, a CI > 1 would suggest a subadditive interaction and a CI < 1 a supra-additive interaction. These calculations resulted in a CI of  $0.57 \pm 0.1$  in T98G cells (Supplementary Fig. S4), which is consistent with the supra-additive interaction between radiation and MK-1775 shown using the traditional clonogenic assay, supporting the potential application of this assay. We therefore extended the clonogenic hybrid to define the interaction of MK-1775 with radiation in astrocytes, which do not grow as colonies. This resulted in a CI of  $1.3 \pm 0.4$ , further supporting the tumor-specific radiosensitization capacity of MK-1775 (Supplementary Fig. S4).

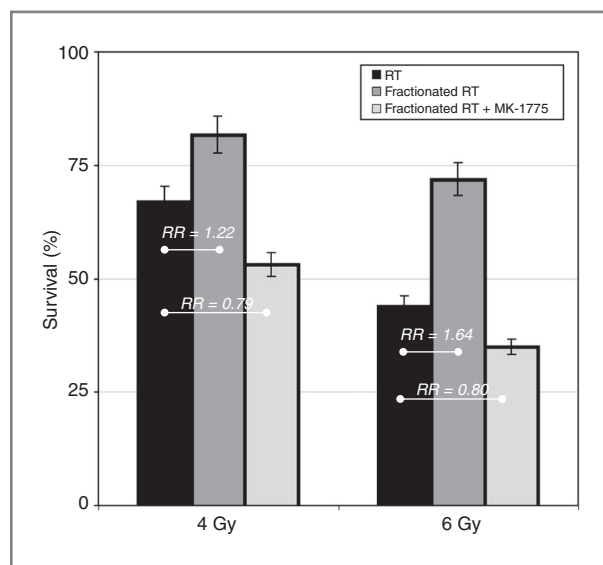


**Figure 4.** MK-1775 attenuates recovery during fractionated radiation. T98G cells were plated, allowed to attach, and exposed to a single fraction of radiation (RT) or fractionated RT (2 Gy every 24 hours) at the stated doses in the presence of MK-1775 (100 nmol/L) or vehicle control. Plates were replaced with fresh culture media after 24 hours (single fraction RT) and 48 and 72 hours for plates treated with 4 and 6 Gy fractionated RT, respectively. Colony survival was determined 10 to 14 days following treatment, normalizing for the independent cytotoxicity of MK-1775. Recovery rates (RR) during fractionated RT were calculated by dividing the percentage of cell survival following fractionated RT by the percentage of cell survival following an equivalent dose of radiation delivered as a single fraction. Mean  $\pm$  SE of 3 independent experiments.

### MK-1775 increases radiation-induced mitotic catastrophe and $\gamma$ H2AX expression

On the basis of the underlying mechanism of action of MK-1775, which involves abrogated radiation-induced cell-cycle arrest and premature entry of cells into mitosis before DNA repair, we went on to determine whether increased induction of mitotic catastrophe was involved in the shown radiosensitization (18). Mitotic cell death, determined by the number of cells with abnormal nuclei (multinuclear giant cells or cells with several micronuclei) was observed following 24-hour exposure to MK-1775 (250 nmol/L) or irradiation (6 Gy) alone in T98G cells. The combination of MK-1775 with irradiation resulted in a supra-additive increase in mitotic catastrophe, statistically greater than either treatment alone (Fig. 5A). These studies were then extended to the GNS line G179 and astrocytes, which, in accordance with the results from the clonogenic assay, showed no interaction of MK-1775 with radiation-induced mitotic catastrophe (Supplementary Fig. S5). Because the underlying rationale for targeting the cell-cycle checkpoint arrest involves an accumulation of unrepaired DNA damage in the cancer cells, the potential for MK-1775 to influence DNA damage repair was determined by evaluating  $\gamma$ H2AX expression using Western blot analysis (6). As shown in Fig. 5B, the combination of MK-1775 and radiation significantly increased  $\gamma$ H2AX expression, beginning 10 hours post-radiation, indicating persistence of unrepaired DNA damage in the tumor cells.

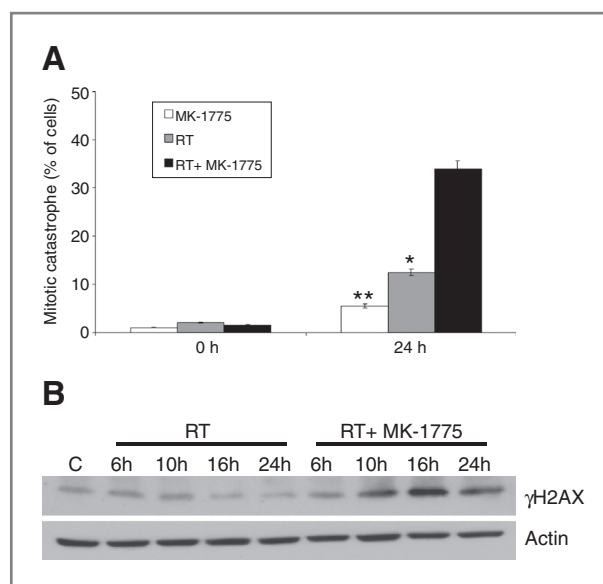


**Figure 5.** MK-1775 augments radiation-induced mitotic catastrophe and  $\gamma$ H2AX expression. **A**, T98G cells growing in chamber slides were exposed to MK-1775 (250 nmol/L) or vehicle control for 6 hours, irradiated (RT, 6 Gy), and fixed at 24 hours post-irradiation for immunocytochemical analysis of mitotic catastrophe. Nuclear fragmentation (defined as the presence of 2 or more distinct lobes within a single cell) was evaluated in 100 cells per treatment per experiment. Mean  $\pm$  SE (\*,  $P = 0.03$ ; \*\*,  $P = 0.001$ ). **B**, T98G cells were treated in the above described conditions, and cell lysates obtained at the indicated times were resolved in SDS-PAGE and probed with specific antibodies against the indicated proteins.

### Wee-1 expression in normal astrocytes and glioblastoma cell lines

Recent work showed the potential of *Wee-1* gene expression levels to correlate with the radiosensitization capacity of *Wee-1* inhibition (12). We therefore extended our work to determine *Wee-1* protein expression levels in our glioblastoma models. As shown in Supplementary Fig. S6, the glioblastoma cell lines differentially overexpressed *Wee-1*. As *Wee-1* was highly expressed in G179, which did not show radiosensitization by MK-1775, and had a relative low expression in T98G, which showed strong radiosensitization, overall expression of *Wee-1* did not appear to predict the capacity of MK-1775 radiosensitization. However, of particular interest, we did not detect any expression of *Wee-1* in astrocytes, further supporting the potential of MK-1775 to serve as a tumor-specific radiosensitizer.

### MK-1775 achieves biologically relevant concentrations *in vivo* and increases radiation-induced growth delay

To determine whether the enhancement of tumor cell radiosensitivity measured *in vitro* could be translated into an *in vivo* tumor model, a tumor growth delay assay using U251 cells grown subcutaneously in the hind leg of nude mice was used. Before proceeding with growth delay

studies, pharmacokinetic studies were conducted to confirm that biologically relevant concentrations of MK-1775 were achievable *in vivo*. For these studies, we chose an MK-1775 dose of 60 mg/kg, which we previously determined to be a safe dose in mice and correlates to clinically relevant doses used in ongoing clinical trials (19). Pharmacokinetic analysis of blood samples shows transient exposure of MK-1775 following a single oral dose of 60 mg/kg, reaching a mean concentration of 2.1  $\mu$ mol/L 1 hour after dosing but dropping to undetectable levels by 10 hours (Supplementary Fig. S7).

On the basis of the relatively short half-life of MK-1775 in mice, a twice-a-day dosing regimen was chosen for further *in vivo* work. For the tumor growth delay assay, mice bearing subcutaneous xenografts were randomized into 4 groups: vehicle, MK-1775 only (60 mg twice daily  $\times$  3 days), fractionated radiation only (2 Gy  $\times$  3 days), or the MK-1775/fractionated radiation combination. For each group, the absolute growth delay was calculated, which equaled the time in days for tumors in treated mice to grow from 125 to 750 mm<sup>3</sup> minus the time in days for tumors to reach the same size in control mice. The absolute growth delay for mice treated with MK-1775 and radiation individually was 2.2 and 7.0 days, respectively. However, in mice that received the MK-1775/fractionated radiation combination, the absolute growth delay was 11.9 days, which was more than the sum of the growth delays caused by MK-1775 alone and radiation alone and statistically significant when compared with the individual treatment arms (radiation alone:  $P = 0.04$ ; MK-1775 alone:  $P = 0.001$ ; Fig. 6A).

### MK-1775 increases mitotic ratio *in vivo*

To determine whether the *in vitro* mechanism of action of MK-1775, involving the attenuation of the G<sub>2</sub> checkpoint arrest leading to an increased mitotic fraction following irradiation, applied *in vivo*, immunohistochemical staining was conducted on tumor xenografts following irradiation, probing for phosphorylated histone H3. Entire sections were then scanned (Supplementary Fig. S8) and mitotic cells quantified using an automated system (Supplementary Fig. S8, inset). A mitotic ratio was then calculated, which equaled the percentage of mitotic cells in the treatment group divided by the control group. Similar to *in vitro* findings, irradiating xenografts resulted in a reduction in mitotic ratio, reflecting the onset of G<sub>2</sub> arrest. Treating mice with MK-1775 attenuated the reduction in mitotic ratio following irradiation (Fig. 6B), supporting this potential of the compound of abrogating radiation-induced G<sub>2</sub> arrest *in vivo*.

### Discussion

Concerted efforts are currently underway to further clinical gains in glioblastoma. As radiation therapy continues to be central to definitive treatment, identifying agents that show the capacity to enhance radiation response holds therapeutic promise in this otherwise

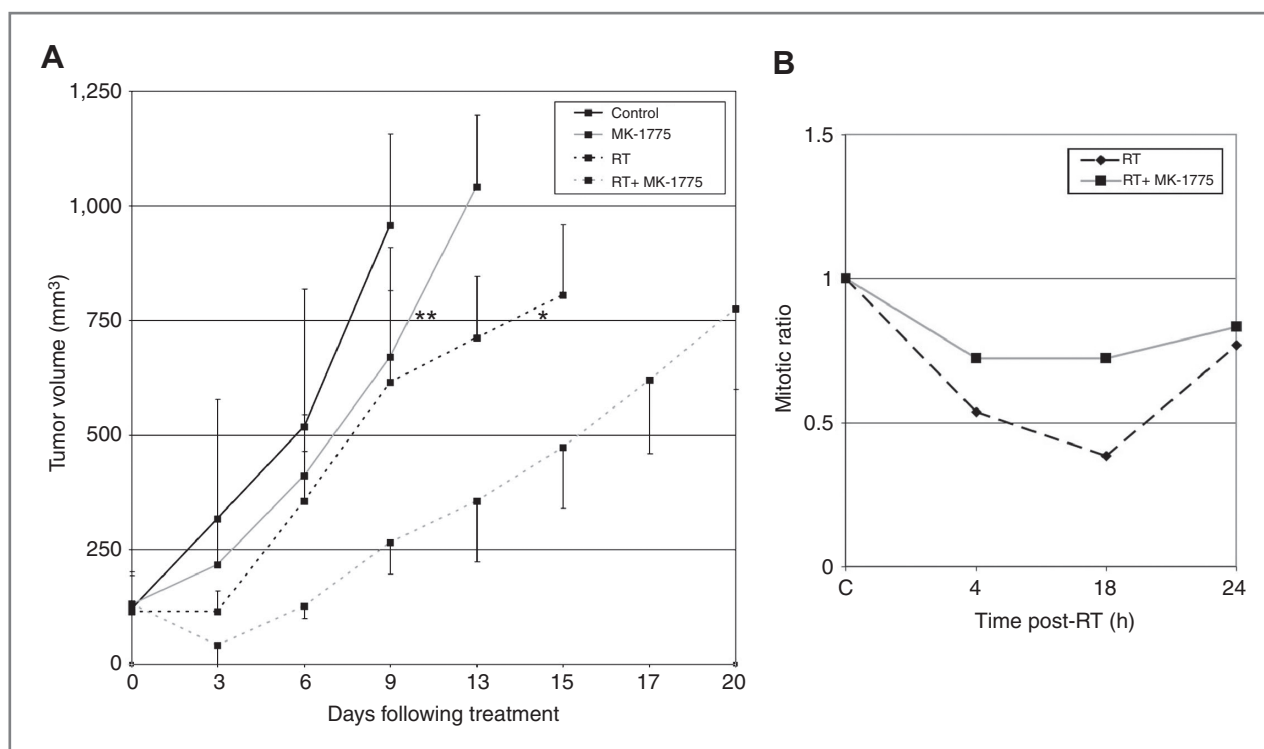


**Figure 6.** MK-1775 enhances radiation-induced tumor growth delay and attenuates the radiation-induced G<sub>2</sub> checkpoint arrest *in vivo*. A, U251 cells were injected subcutaneously in a mouse flank model. When tumors reached about 150 mm<sup>3</sup> in size, mice were randomized into 4 groups: vehicle control, MK-1775 (60 mg/kg twice daily × 3 days), irradiation (2 Gy × 3 days; RT), or MK-1775 + irradiation. To obtain a tumor growth curve, perpendicular diameter measurements of each tumor were measured with digital calipers, and volumes were calculated using formula  $(L \times W \times H)/2$ . Each group contained 7 mice (\*, RT vs. RT + MK-1775:  $P = 0.04$ ; \*\*, MK-1775 vs. RT + MK-1775:  $P = 0.001$ ). Mean ± SE. B, U251 cells were injected subcutaneously in a mouse flank model. When tumors reached about 500 mm<sup>3</sup> in size, mice were randomized into 3 groups: vehicle control, irradiation (6 Gy; RT), or MK-1775 (60 mg/kg twice daily, beginning 2 hours before RT) + irradiation (6 Gy). At the stated times, animals were sacrificed and tumors were removed, formalin fixed, and paraffin embedded. Immunohistochemical staining was conducted to determine the mitotic ratio by immunostaining for phospho-histone H3 expression. The entire section was then quantified using an automated system and mitotic ratio calculated, which equaled the percentage of mitotic cells in the treatment group divided by the control group.

deadly malignancy. On the basis of this rationale, several molecularly targeted agents have shown the potential to serve as radiosensitizers and are currently being tested clinically. However, because these growth and signaling pathways also influence radiation response in normal cells, the potential of these agents to also sensitize normal tissue to radiation, thereby mitigating their improvement in therapeutic index, is a clear possibility. Because normal cells typically rely on the G<sub>1</sub> checkpoint to repair DNA following double-strand breaks, targeting the G<sub>2</sub> checkpoint may represent a unique opportunity for tumor-specific radiosensitization. In this study, we tested the potential of the Wee-1 inhibitor MK-1775 to target the G<sub>2</sub> checkpoint and modulate radiation response in a panel of glioblastoma cell lines and normal astrocytes. In established glioblastoma cell lines, MK-1775 showed a dose-dependent attenuation of the radiation-induced G<sub>2</sub> checkpoint arrest and increase in radiosensitization. These findings are consistent with previous investigations identifying the potential of Wee-1 to serve as a molecular target for radiosensitization (12, 20, 21). Although there was a modest DEF when evaluating noncytotoxic concentra-

tions of MK-1775, the clinical potential of this combination may be better appreciated when studying recovery rate following the more clinically relevant delivery of fractionated radiation. Our *in vitro* studies suggest an equivalent cytotoxicity in T98G cells when 2 Gy is delivered in 3 daily fractions with MK-1775 when compared with 6 Gy delivered as a single fraction; which, if tumor specific, as our data suggest, may have important clinical implications. These *in vitro* results were further supported by *in vivo* findings using a subcutaneous model. However, one limitation to this work is that it does not assess the capacity of this agent to cross the blood-brain barrier. Therefore, further preclinical work using an orthotopic glioblastoma model, along with phase 0 clinical trials determining the concentrations of MK-1775 in tumor tissue will be important to better determine its clinical application in glioblastoma.

We went on to explore the potential mechanism(s) underlying the favorable interaction between MK-1775 and radiation in our models. As cell-cycle checkpoint activation is a critical mediator allowing cells to repair DNA damage before mitotic entry, we first confirmed the



capacity of MK-1775 to push cells through mitosis following irradiation both *in vitro* and *in vivo*, as measured by the mitosis-specific marker phosphorylated histone H3. This resulted in a supra-additive increase in mitotic catastrophe, representing a dominant mode of cell killing following irradiation and unrepaired DNA damage, which is in accord with recent work involving the Wee-1 inhibitor PD0166285 in glioblastoma lines (12).

Because the G<sub>1</sub> checkpoint arrest requires functional p53, tumors harboring p53 mutations may be particularly reliant on the G<sub>2</sub> arrest, thereby serving as a putative biomarker for Wee-1 inhibitors. Although a direct link between p53 function and radiosensitization following Wee-1 inhibition has been defined using p53-specific constructs (20, 21), our findings, along with work recently presented by Mir and colleagues (12), show the potential for this class of agents to also augment radiation response in p53 wild-type glioblastoma lines. This appears to be consistent with recent findings from the Cancer Genome Atlas (10), which identified that in addition to p53 mutation, an overwhelming majority of glioblastoma harbor mutations in genes involved in the p53 signaling pathway. This suggests a reliance on the G<sub>2</sub> checkpoint following DNA damage, despite functional p53 in a large proportion of glioblastoma. Mir and colleagues (12) went on to identify *Wee-1* gene expression as potential biomarker for radiosensitization following Wee-1 inhibition; however, this correlation did not seem to translate when protein expression was evaluated in our models. Potential differences between mRNA and protein levels of Wee-1, along with the target specificity of individual agents used in the 2 studies may underlie these discordant results. However, we did identify that NHAs have very little expression of Wee-1 when compared with the glioblastoma lines, which suggests this protein may play a role in glioblastoma tumorigenesis and further supports the tumor-specific radiosensitization potential of these agents.

Although MK-1775 showed consistent radiosensitization in established glioblastoma cell lines, it did not appear to significantly modulate radiation response in the GNS cell models used in this study, despite these lines showing a robust G<sub>2</sub> checkpoint response. On the basis of the critical role the DNA damage checkpoint response plays in glioblastoma stem cell biology and therapeutic resistance (17), we studied the temporal dynamics of the cell-

cycle phase distribution in the GNS lines to provide further insight into these unexpected findings. The early-phase of the G<sub>2</sub> checkpoint appears to be Wee-1 dependent, with both GNS cell lines showing an attenuated radiation-induced G<sub>2</sub> phase accumulation when treated with MK-1775, similar to established glioblastoma cell lines. However, this arrest was not sustained during the late-phase response, with GNS cells rapidly accumulating and sustaining a G<sub>2</sub> arrest 16 and 24 hours following irradiation, suggesting that this late-phase response may be activated through a Wee-1-independent signaling pathway. These findings are in accord with previous investigations suggesting that glioblastoma tumor stem cells may be particularly reliant on other proteins for checkpoint activation, including Chk1 and/or Chk2 (17). Although clearly more focused investigations are required to better understand the proteins involved in the dynamic checkpoint response of glioblastoma stem cells, which includes expanding these investigations to other glioblastoma stem cell models and studying *in vivo* response using an orthotopic model, these early findings suggest that although Wee-1 inhibition has broad radiosensitization capacity warranting clinical investigation, targeting this pathway alone may be insufficient to abrogate checkpoint activation in this unique cell population.

#### Disclosure of Potential Conflicts of Interest

P. Chinnaiyan received grant funding from Merck Research Laboratories. S.D. Shumway, Y. Xu, and T. Demuth are employees of Merck. No potential conflicts of interest were disclosed by other authors.

#### Acknowledgments

The authors thank John Schriener, PhD, for his assistance in project development.

#### Grant Support

This project was supported by Merck Research Laboratories and the Ben and Catherine Ivy Foundation to P. Chinnaiyan.

The costs of publication of this article were defrayed in part by the payment of page charges. This article must therefore be hereby marked *advertisement* in accordance with 18 U.S.C. Section 1734 solely to indicate this fact.

Received June 27, 2011; revised September 21, 2011; accepted September 24, 2011; published OnlineFirst October 12, 2011.

#### References

- Milano MT, Okunieff P, Donatello RS, Mohile NA, Sul J, Walter KA, et al. Patterns and timing of recurrence after temozolomide-based chemoradiation for glioblastoma. *Int J Radiat Oncol Biol Phys* 2010;78:1147–55.
- Rowley R, Hudson J, Young PG. The *wee1* protein kinase is required for radiation-induced mitotic delay. *Nature* 1992;356:353–5.
- Kawabe T. G<sub>2</sub> checkpoint abrogators as anticancer drugs. *Mol Cancer Ther* 2004;3:513–9.
- Rhind N, Russell P. Roles of the mitotic inhibitors Wee1 and Mik1 in the G<sub>2</sub> DNA damage and replication checkpoints. *Mol Cell Biol* 2001;21:1499–508.
- Xu B, Kim ST, Lim DS, Kastan MB. Two molecularly distinct G<sub>2</sub>/M checkpoints are induced by ionizing irradiation. *Mol Cell Biol* 2002;22:1049–59.
- Rajeshkumar NV, De Oliveira E, Ottenhof N, Watters JW, Brooks D, Demuth T, et al. MK-1775, a potent Wee1 inhibitor, synergizes with gemcitabine to achieve tumor regressions, selectively in p53-deficient pancreatic cancer xenografts. *Clin Cancer Res* 2011;17:2799–806.
- Lundgren K, Walworth N, Booher R, Dembski M, Kirschner M, Beach D. *mik1* and *wee1* cooperate in the inhibitory tyrosine phosphorylation of *cdc2*. *Cell* 1991;64:1111–22.

8. Hirai H, Iwasawa Y, Okada M, Arai T, Nishibata T, Kobayashi M, et al. Small-molecule inhibition of Wee1 kinase by MK-1775 selectively sensitizes p53-deficient tumor cells to DNA-damaging agents. *Mol Cancer Ther* 2009;8:2992–3000.
9. Zheng H, Ying H, Yan H, Kimmelman AC, Hiller DJ, Chen AJ, et al. p53 and Pten control neural and glioma stem/progenitor cell renewal and differentiation. *Nature* 2008;455:1129–33.
10. Cancer Genome Atlas Research Network. Comprehensive genomic characterization defines human glioblastoma genes and core pathways. *Nature* 2008;455:1061–8.
11. Hirai H, Arai T, Okada M, Nishibata T, Kobayashi M, Sakai N, et al. MK-1775, a small molecule Wee1 inhibitor, enhances anti-tumor efficacy of various DNA-damaging agents, including 5-fluorouracil. *Cancer Biol Ther* 2010;9:514–22.
12. Mir SE, De Witt Hamer PC, Krawczyk PM, Balaj L, Claes A, Niers JM, et al. *In silico* analysis of kinase expression identifies WEE1 as a gatekeeper against mitotic catastrophe in glioblastoma. *Cancer Cell* 2011;18:244–57.
13. Pollard SM, Yoshikawa K, Clarke ID, Danovi D, Stricker S, Russell R, et al. Glioma stem cell lines expanded in adherent culture have tumor-specific phenotypes and are suitable for chemical and genetic screens. *Cell Stem Cell* 2009;4:568–80.
14. Kahali S, Sarcar B, Fang B, Williams ES, Koomen JM, Tofilon PJ, et al. Activation of the unfolded protein response contributes toward the antitumor activity of vorinostat. *Neoplasia* 2010;12:80–6.
15. Dirks PB. Brain tumor stem cells: bringing order to the chaos of brain cancer. *J Clin Oncol* 2008;26:2916–24.
16. Singh SK, Hawkins C, Clarke ID, Squire JA, Bayani J, Hide T, et al. Identification of human brain tumour initiating cells. *Nature* 2004;432:396–401.
17. Bao S, Wu Q, McLendon RE, Hao Y, Shi Q, Hjelmeland AB, et al. Glioma stem cells promote radioresistance by preferential activation of the DNA damage response. *Nature* 2006;444:756–60.
18. Castedo M, Perfettini JL, Roumier T, Andreau K, Medema R, Kroemer G. Cell death by mitotic catastrophe: a molecular definition. *Oncogene* 2004;23:2825–37.
19. Reagan-Shaw S, Nihal M, Ahmad N. Dose translation from animal to human studies revisited. *FASEB J* 2008;22:659–61.
20. Li J, Wang Y, Sun Y, Lawrence TS. Wild-type TP53 inhibits G(2)-phase checkpoint abrogation and radiosensitization induced by PD0166285, a WEE1 kinase inhibitor. *Radiat Res* 2002;157:322–30.
21. Wang Y, Li J, Booher RN, Kraker A, Lawrence T, Leopold WR, et al. Radiosensitization of p53 mutant cells by PD0166285, a novel G(2) checkpoint abrogator. *Cancer Res* 2001;61:8211–7.

# Molecular Cancer Therapeutics

## Targeting Radiation-Induced G<sub>2</sub> Checkpoint Activation with the Wee-1 Inhibitor MK-1775 in Glioblastoma Cell Lines

Bhaswati Sarcar, Soumen Kahali, Antony H. Prabhu, et al.

*Mol Cancer Ther* 2011;10:2405-2414. Published OnlineFirst October 12, 2011.

**Updated version** Access the most recent version of this article at:  
doi:[10.1158/1535-7163.MCT-11-0469](https://doi.org/10.1158/1535-7163.MCT-11-0469)

**Supplementary Material** Access the most recent supplemental material at:  
<http://mct.aacrjournals.org/content/suppl/2011/10/04/1535-7163.MCT-11-0469.DC1>

**Cited articles** This article cites 21 articles, 7 of which you can access for free at:  
<http://mct.aacrjournals.org/content/10/12/2405.full#ref-list-1>

**Citing articles** This article has been cited by 15 HighWire-hosted articles. Access the articles at:  
<http://mct.aacrjournals.org/content/10/12/2405.full#related-urls>

**E-mail alerts** [Sign up to receive free email-alerts](#) related to this article or journal.

**Reprints and Subscriptions** To order reprints of this article or to subscribe to the journal, contact the AACR Publications Department at [pubs@aacr.org](mailto:pubs@aacr.org).

**Permissions** To request permission to re-use all or part of this article, use this link  
<http://mct.aacrjournals.org/content/10/12/2405>.  
Click on "Request Permissions" which will take you to the Copyright Clearance Center's (CCC) Rightslink site.